Noname manuscript No.
(will be inserted by the editor)

A Control Method for Joint Torque Minimization of Redundant Manipulators Handling Large External Forces

Jonathan Woolfrey · Wenjie Lu · Dikai Liu

Received: date / Accepted: date

Abstract In this paper, a control method is developed for minimizing joint torque on a redundant manipulator where an external force acts on the end-effector. Using null space control, the redundant task is designed to minimize the torque needed to oppose the external force, and reduce the dynamic torque. Furthermore, the joint motion can be weighted to factor in physical constraints such as joint limits, collision avoidance, etc. Conventional methods for joint torque minimization only consider the internal dynamics of the manipulator. If external forces acting on the end-effector are inadvertently implemented in to these control methods this could lead to joint configurations that amplify the resulting joint torque. The proposed control method is verified through two different case studies. The first case study involves simulation of high-pressure blasting. The second is a simulation of a manipulator lifting and moving a heavy object. The results show that the proposed control method reduces overall joint torque compared to conventional methods. Furthermore, the joint torque is minimized such that there is potential for a manipulator to execute certain tasks beyond its nominal payload capacity.

Keywords null space control · dynamic control · optimization · robotic manipulator · redundancy · torque minimization

1 Introduction

The utility of robotic manipulators is their ability to carry out laborious tasks that involve interactions with objects, or negotiating with various external forces. This can include tasks such as lifting, pushing/pulling, bracing the manipulator against external shocks, or carrying out high-pressure blasting for cleaning surfaces. External forces on the end-effector introduce additional joint torque alongside the

J. Woolfrey
University of Technology Sydney
81 Broadway, Ultimo, 2007, NSW, Australia
Tel.: +61 2 9514 2588
Fax: +61 2 9514 1810
E-mail: jonathan.woolfrey@student.uts.edu.au

internal dynamic torque during task execution. Furthermore, there may be cases in which the manipulator is required to work at or above its nominal payload capacity. In such instances, careful control of the joint configuration is necessary to keep joint torques within appropriate limits.

For instance, a robotic system has been previously developed for grit-blasting of the iconic Sydney Harbour Bridge at the University of Technology Sydney (UTS) [1]. The Denso VM manipulator was originally used, which has an advertised payload capacity of 13 kg (and specific end-effector pose requirements at 11kg of loading) [2]. The nozzle reaction forces reached a magnitude of 106N (10.8kg) due to the high fluid velocities involved. Consequently, there were noted control issues during field experiments due to the heavily laden manipulator [3]. A large manipulator was initially chosen to cope with the high payload requirements. However, this conflicted with the restrictions on size due to the confined workspaces it had to operate in [1]. The mass of the manipulator was also raised as an issue, due to the frequency with which it had to be repositioned in the environment [4]. Some research had been conducted in anticipation of the large payload forces [6]. Ideally, a light-weight robot manipulator with very high payload is needed for applications in complex and unstructured environments.

New research is also being conducted in to an autonomous underwater vehicle-manipulator system (AUVMS) capable of high-pressure water cleaning of submerged infrastructure [5, 7]. Many current AUVMS have heavy manipulators mounted beneath the vehicle body to assist with passive stability. Conversely, a light-weight, top-mounted manipulator is needed for underwater cleaning robots to meet task, logistics, and stability requirements. Generally, the payload capacity of a manipulator must be balanced against other requirements such as size, weight, workspace volume, dexterity, and degrees of freedom [8]. As such, it is not always possible to increase payload capacity without sacrificing other performance measures. Therefore, prudent control of the manipulator can reduce joint torque required for the task given these constraints.

Redundant manipulators have more degrees of freedom than required by the primary task (typically the end-effector control). As such, they are capable of self-motion that will not affect said task. This enables them to achieve secondary performance criteria without impeding the main (or higher priority) task [9]. This property has been utilized in previous literature to reduce torque to track a given end-effector trajectory [10-17]. However, these methods reduce joint torque through local optimization of the internal system dynamics. Applying these control methods to tasks with forces on the end-effector may lead to configurations that exacerbate the torque in the long term.

Some of the earliest work on torque minimization in literature can be found in [10]. The authors proposed a control method that utilized redundancy to locally minimize kinetic energy and avoid joint torque limits. In [11], it was shown that the minimum torque norm, weighted by the inverse of the inertia matrix, leads to a global reduction in kinetic energy in the manipulator. For future reference, this is referred to as the Minimum Kinetic Energy (MKE) method. In both cases, it was noted that dynamic level control of redundant manipulators can lead to instability in the system over long periods. This lead to the authors of [12] to devise the null space damping method. This method exponentially slows joints in the null space of the manipulator. It was also noted that the null space damping method outperforms previous methods in terms of joint torque minimization.

In [13], a method for damping joint torques in the presence of kinematic singularities was proposed. As in [12], the authors also used null space damping to ensure global stability of the system. Machine learning has also been explored for joint torque optimization [14]. Neural networks were used to generate control torques to track a given end-effector trajectory, whilst remaining bounded by the joint torque limits. More recently, quadratic programming (QP) has been used to address the minimization problem with consideration for joint, velocity, and acceleration constraints [15, 16]. The latter used simultaneous torque and velocity minimization. This method circumvented high joint velocities in the null space that lead to instability problems as observed in [10-12]. The authors in [17] developed a method of discrete-time velocity control that incorporated torque optimization properties. As aforementioned, these methods are devised with respect to the manipulators internal dynamics and physical constraints. The objective here is to minimize the torque of a redundant manipulator where an external force is applied to the end-effector (i.e. a wrench). High-pressure blasting makes for an interesting case study, as the force vector continually changes with the direction of the nozzle.

The paper is organized as follows. In Section II, the problem formulation is given with respect to the kinematics and dynamics of a serial link manipulator. Section III presents the conventional method for joint torque minimization. In particular, the inverse-inertia weighted torque norm control is considered because of its well-known property of kinetic energy minimization [11]. This method is also used as a baseline to compare with the torque minimization method devised in this paper.

Section IV contains a review of methods for stabilizing redundant manipulators at the acceleration/torque level, using null space damping, and null space control. Using the latter, it is possible to control the redundant portion of the manipulator to achieve secondary performance criteria. This is the basis from which the proposed joint torque minimization method will be developed.

In Section V, a new control method is presented for minimizing joint torque resulting from a wrench on the end-effector. The resultant joint motion is based on a Weighted Least Norm (WLN) optimization, which can be used for joint limit and/or collision avoidance [18-20]. In doing so, the manipulator can reconfigure itself to reduce the joint torque loading whilst tracking a trajectory and adhering to physical constraints. The redundant control is also attenuated by the local dynamic torque.

In Section VI, the efficacy of the proposed control method is explored in two different case studies. The first involves a simulation of a manipulator lifting and moving a heavy object. This object is inertially coupled with the manipulator, hence the control method must account for both the torque needed to lift the object, and the system dynamics. The second case study pertains to a simulation of a manipulator performing high-pressure blasting across a given trajectory. In this scenario, the manipulator must continually compensate for the change in forces as the nozzle points in different directions. In both cases, the proposed control method is compared against conventional joint torque minimization methods and is shown to have better performance outcomes.

2 Problem Formulation

2.1 Serial-Link Manipulator Kinematics

The forward kinematics of a serial link manipulator describes the position and orientation of the end-effector as a function of joint angles:

$$\mathbf{x} = \mathbf{f}(\mathbf{q}), \tag{1}$$

where $\mathbf{x} \in \mathbb{R}^{\mathrm{m}}$ is a vector denoting the pose of the end-effector, and $\mathbf{q} \in \mathbb{R}^{\mathrm{n}}$ is a vector of joint angles. Differentiating (1) with respect to time gives:

$$\begin{aligned} \dot{\mathbf{x}} &= \frac{\partial \mathbf{x}}{\partial \mathbf{q}} \dot{\mathbf{q}} \\ &= \mathbf{J}(\mathbf{q})\dot{\mathbf{q}} \qquad (2) \\ \ddot{\mathbf{x}} &= \dot{\mathbf{J}}(\mathbf{q}, \dot{\mathbf{q}})\dot{\mathbf{q}} + \mathbf{J}(\mathbf{q})\ddot{\mathbf{q}}, \qquad (3) \end{aligned}$$

where $\mathbf{J}(\mathbf{q}) \in \mathbb{R}^{\mathrm{m}\times\mathrm{n}}$ is the Jacobian matrix for the manipulator. The vector $\ddot{\mathbf{x}}$ denoting the primary task is the end-effector acceleration required to track a given trajectory. Equation (3) can then be solved for $\ddot{\mathbf{q}}$ using weighted-least-squares with a redundant task $\ddot{\mathbf{z}} \in \mathbb{R}^{\mathrm{n}}$ projected on to the manipulator null space:

$$\ddot{\mathbf{q}} = \mathbf{J}_{\mathrm{W}}^{\dagger}(\ddot{\mathbf{x}} - \dot{\mathbf{J}}\dot{\mathbf{q}}) + \mathbf{N}_{\mathrm{W}}\ddot{\mathbf{z}} \tag{4}$$

$$\mathbf{J}_{\mathrm{W}}^{\dagger} = \mathbf{W}^{-1}\mathbf{J}^{\mathrm{T}}(\mathbf{J}\mathbf{W}^{-1}\mathbf{J}^{\mathrm{T}})^{-1} \tag{5}$$

$$\mathbf{N}_{\mathrm{W}} = \mathbf{I} - \mathbf{J}_{\mathrm{W}}^{\dagger}\mathbf{J}, \tag{6}$$

with $\mathbf{J}_{\mathrm{W}}^{\dagger}$ being the weighted Moore-Penrose pseudoinverse Jacobian, $\mathbf{N}_{\mathrm{W}}$ the null space matrix, and $\mathbf{W}$ a positive-definite weighting matrix. Note that multiplying (4) by the Jacobian gives $\mathbf{J}\ddot{\mathbf{q}} = \ddot{\mathbf{x}} - \dot{\mathbf{J}}\dot{\mathbf{q}}$ and hence the kinematic relationship in (3) is preserved. The task defined by $\ddot{\mathbf{z}}$ with have no effect on the end-effector motion.

In some instances, (5) becomes ill-conditioned as the manipulator approaches a singularity. The pseudoinverse Jacobian can be modified using the well-known Damped-Least-Squares (DLS) approach [21]:

$$\mathbf{J}_{\mathrm{W,DLS}}^{\dagger} = \mathbf{W}^{-1}\mathbf{J}^{\mathrm{T}}(\mathbf{J}\mathbf{W}^{-1}\mathbf{J}^{\mathrm{T}} - \lambda\mathbf{I})^{-1}, \tag{7}$$

where λ is a scalar damping coefficient. This can be attenuated based on proximity to a singular configuration to mitigate task error [22].

2.2 Manipulator Dynamics

From a desired joint acceleration (4), the subsequent joint torques can be calcuated from the manipulator dynamics:

$$\boldsymbol{\tau} = \mathbf{M}(\mathbf{q})\ddot{\mathbf{q}} + \mathbf{c}(\mathbf{q}, \dot{\mathbf{q}}) + \mathbf{g}(\mathbf{q}) + \boldsymbol{\tau}_{\mathrm{R}}(\mathbf{q}) \tag{8}$$

where:

- $\mathbf{M}(\mathbf{q})$ is the inertia matrix,
- $\mathbf{c}(\mathbf{q}, \dot{\mathbf{q}})$ is the vector of Coriolis and centripetal torques,
- $\mathbf{g}(\mathbf{q})$ is the gravity torque vector,
- and $\boldsymbol{\tau}_{\mathrm{R}}(\mathbf{q})$ is a vector of joint torques contributed from an external load on the end-effector.

The vector of joint torques produced from a wrench on the end-effector can be calculated from the manipulator Jacobian. Assuming a static configuration, and for some infinitesimally small displacements of $\Delta\mathbf{x}$ and $\Delta\mathbf{q}$, it holds that:

$$\Delta\mathbf{x} = \mathbf{J}\Delta\mathbf{q}. \tag{9}$$

Then from the principle of virtual work, the change in total energy of the system must be zero:

$$\Delta\mathrm{E} = \boldsymbol{\nu}_0^{\mathrm{T}}\Delta\mathbf{x} - \boldsymbol{\tau}_{\mathrm{R}}^{\mathrm{T}}\Delta\mathbf{q} = 0, \tag{10}$$

where $\boldsymbol{\tau}_{\mathrm{R}}$ is a vector of torques needed to oppose a wrench on the end-effector $\boldsymbol{\nu}_0$, specified in the base frame $\{0\}$. Substituting (9) in (10), and solving for $\boldsymbol{\tau}_{\mathrm{R}}$:

$$\begin{aligned} \boldsymbol{\nu}_0\mathbf{J}\Delta\mathbf{q} &= \boldsymbol{\tau}_{\mathrm{R}}^{\mathrm{T}}\Delta\mathbf{q} \\ \boldsymbol{\tau}_{\mathrm{R}} &= \mathbf{J}^{\mathrm{T}}\boldsymbol{\nu}_0 \\ &= \mathbf{J}^{\mathrm{T}}\mathbf{R}_{\mathrm{i}}\boldsymbol{\nu}_{\mathrm{i}} \end{aligned} \tag{11}$$

$$\mathbf{R}_{\mathrm{i}} = \begin{bmatrix} \mathbf{R}_0^{\mathrm{i}}(\mathbf{q}) & \mathbf{0}_{3\times3} \\ \mathbf{0}_{3\times3} & \mathbf{R}_0^{\mathrm{i}}(\mathbf{q}) \end{bmatrix}, \tag{12}$$

where $\mathbf{R}_0^{\mathrm{i}}(\mathbf{q}) \in \mathbb{SO}(3)$ being a transformation from the manipulator base frame 0 to some other frame i. It is evident from (11) that the joint torques needed to oppose an external loading on the manipulator is dependent on the joint configuration $\mathbf{q}$. By using redundancy in the system, it is possible to reconfigure the joints to reduce the magnitude of the torque vector $\boldsymbol{\tau}_{\mathrm{R}}$.

From (3), if $\mathrm{n} > \mathrm{m}$ there are infinite joint motions that can achieve the desired primary task. As such, the objective here is to find a joint acceleration $\ddot{\mathbf{q}}$ to achieve two objectives. Firstly, to track the end-effector trajectory. Secondly, to minimize the torque required torque to achieve it. This comprises both the torque needed to oppose a force on the end-effector, and the dynamic torque required to move the manipulator.

3 Conventional Methods for Torque Minimization

A common approach in literature for dynamic torque optimization is the MKE method [11, 12, 14, 15]. This method solves a constrained optimization problem at each time step of the form:

$$\begin{aligned} &\min_{\ddot{\mathbf{q}}} \frac{1}{2}\boldsymbol{\tau}^{\mathrm{T}}\mathbf{M}^{-1}\boldsymbol{\tau} \\ &\text{subject to } \ddot{\mathbf{x}} - \dot{\mathbf{J}}\dot{\mathbf{q}} - \mathbf{J}\ddot{\mathbf{q}} = \mathbf{0}. \end{aligned} \tag{13}$$

By substituting (8) in to (13), and solving using the method of Lagrange multipliers, the solution is:

$$\ddot{\mathbf{q}} = \mathbf{J}_{\mathrm{M}}^{\dagger}(\ddot{\mathbf{x}} - \dot{\mathbf{J}}\dot{\mathbf{q}}) - \mathbf{N}_{\mathrm{M}}\mathbf{M}^{-1}(\mathbf{c} + \boldsymbol{\tau}_{\mathrm{R}}). \tag{14}$$

This solution is equivalent to (4) in which $\mathbf{W} \equiv \mathbf{M}$, and $\ddot{\mathbf{z}} \equiv \mathbf{M}^{-1}(\mathbf{c} + \boldsymbol{\tau}_{\mathrm{R}})$. As in [11], the gravity torque $\mathbf{g}$ has been removed. This way, the manipulator configuration does not droop as it attempts to reduce the gravitational potential energy in the system. Furthermore, the original formulation did not include the term $\boldsymbol{\tau}_{\mathrm{R}}$. It is shown in [11] that (14), sans $\boldsymbol{\tau}_{\mathrm{R}}$, leads to a global minimization of kinetic energy in the manipulator system. This will be used as a baseline to compare with the control method developed in this paper.

The MKE method was originally devised with respect to the dynamic torque. The introduction of an external force/torque $\boldsymbol{\tau}_{\mathrm{R}}$ in to this control as in (14) does not always lead to a reduction in the total joint torque in the long term. This can be seen from simulation results in Section 6. Furthermore, physical constraints on the system are not accounted for. Some QP methods for joint torque minimization exist that include inequality constraints on joint angles, joint velocity, and joint torque [15, 16]. As with [11], the authors only considered dynamic joint torque minimization. A disadvantage to these QP methods is that they lack a closed-form solution.

4 Null Space Stability and Control

The control equations for a redundant manipulator should be carefully formulated at the acceleration level else the null space velocities remain uncontrolled. That is, any combination of joints not contributing to the end-effector motion can move freely which can make the system unstable. Two methods are proposed in literature to address this problem. The first is the null space damping method [12]. This was used to modify the MKE method of torque minimization to achieve stability. The second is null space velocity control [23], which will be used later to reduce torque from an external loading whilst the end-effector tracks a given trajectory.

4.1 Stabilization via the Null Space Damping Method

To address the problem of instability, a damping term can be appended to (14):

$$\ddot{\mathbf{q}} = \mathbf{J}_{\mathrm{M}}^{\dagger}(\ddot{\mathbf{x}} - \dot{\mathbf{J}}\dot{\mathbf{q}}) - \mathbf{N}_{\mathrm{M}}(\mathbf{M}^{-1}(\mathbf{c} + \boldsymbol{\tau}_{\mathrm{R}}) + \beta\dot{\mathbf{q}}), \tag{15}$$

for some scalar $\beta > 0$. Thus, any uncontrolled joints in the null space will slow down exponentially [12].

4.2 Stabilization via Null Space Velocity Control

To address null space instability, the authors in [23] devised a method to control the null space velocities to a desired state. The advantage with this method is the ability to optimize a performance criterion as a function of the joint state, much like [9]. The control scheme is briefly presented here, and in Section 5 the framework is applied to simultaneously minimize torque for trajectory tracking whilst incorporating physical system constraints. First, the control accelerations can be defined as:

$$\ddot{\mathbf{q}} = \mathbf{J}^{\dagger}(\ddot{\mathbf{x}} - \dot{\mathbf{J}}\dot{\mathbf{q}}) + \ddot{\mathbf{z}}_{\mathrm{N}}, \tag{16}$$

where $\ddot{\mathbf{z}}_{\mathrm{N}} \in \mathbb{R}^{\mathrm{n}}$ is a redundant task such that $\mathbf{J}\ddot{\mathbf{z}}_{\mathrm{N}} = \mathbf{0}$, and $\mathbf{J}^{\dagger}$ is the unweighted Moore-Penrose pseudoinverse Jacobian. To control the null space velocities, the following was proposed [23]:

$$\ddot{\mathbf{z}}_{\mathrm{N}} = \mathbf{N}(\ddot{\mathbf{q}}_{\mathrm{d}} + \mathbf{K}_{\mathrm{N}}\mathbf{e}_{\mathrm{N}}) - (\dot{\mathbf{J}}^{\dagger} + \mathbf{J}^{\dagger}\dot{\mathbf{J}}\mathbf{J}^{\dagger})\mathbf{J}(\dot{\mathbf{q}}_{\mathrm{d}} - \dot{\mathbf{q}}), \tag{17}$$

where $\dot{\mathbf{q}}_{\mathrm{d}}$ is the desired joint velocity, and $\mathbf{N}$ is the unweighted null space matrix; $\mathbf{N} \equiv \mathbf{N}_{\mathrm{W}}$ for $\mathbf{W} = \mathbf{I}$ (6), $\mathbf{K}_{\mathrm{N}}$ is a positive-definite gain matrix, and $\mathbf{e}_{\mathrm{N}}$ is the null space velocity error:

$$\mathbf{e}_{\mathrm{N}} = \mathbf{N}(\dot{\mathbf{q}}_{\mathrm{d}} - \dot{\mathbf{q}}). \tag{18}$$

By taking the time derivative of (18), and substituting in (16) and (17):

$$\begin{aligned}
\dot{\mathbf{e}}_{\mathrm{N}} &= \mathbf{N}(\ddot{\mathbf{q}}_{\mathrm{d}} - \ddot{\mathbf{q}}) - \mathbf{J}^{\dagger}\dot{\mathbf{J}}\mathbf{e}_{\mathrm{N}} - (\dot{\mathbf{J}}^{\dagger} + \mathbf{J}^{\dagger}\dot{\mathbf{J}}\mathbf{J}^{\dagger})\mathbf{J}(\dot{\mathbf{q}}_{\mathrm{d}} - \dot{\mathbf{q}}) && (19)\\
&= \mathbf{N}(\ddot{\mathbf{q}}_{\mathrm{d}} - \ddot{\mathbf{z}}_{\mathrm{N}}) - \mathbf{J}^{\dagger}\dot{\mathbf{J}}\mathbf{e}_{\mathrm{N}} - (\dot{\mathbf{J}}^{\dagger} + \mathbf{J}^{\dagger}\dot{\mathbf{J}}\mathbf{J}^{\dagger})\mathbf{J}(\dot{\mathbf{q}}_{\mathrm{d}} - \dot{\mathbf{q}}) && (20)\\
&= -\mathbf{N}\mathbf{K}_{\mathrm{N}}\mathbf{e}_{\mathrm{N}} - \mathbf{J}^{\dagger}\dot{\mathbf{J}}\mathbf{e}_{\mathrm{N}}. && (21)
\end{aligned}$$

A Lyapunov candidate function can be defined as the sum-of-squared errors:

$$\mathrm{V} = \frac{1}{2}\mathbf{e}_{\mathrm{N}}^{\mathrm{T}}\mathbf{e}_{\mathrm{N}}, \tag{22}$$

then the time-derivative is:

$$\begin{aligned}
\dot{\mathrm{V}} &= \mathbf{e}_{\mathrm{N}}^{\mathrm{T}}\dot{\mathbf{e}}_{\mathrm{N}}\\
&= -\mathbf{e}_{\mathrm{N}}^{\mathrm{T}}\mathbf{N}\mathbf{K}_{\mathrm{N}}\mathbf{e}_{\mathrm{N}} - \mathbf{e}_{\mathrm{N}}^{\mathrm{T}}\mathbf{J}^{\dagger}\dot{\mathbf{J}}\mathbf{e}_{\mathrm{N}}\\
&= -\mathbf{e}_{\mathrm{N}}^{\mathrm{T}}\mathbf{K}_{\mathrm{N}}\mathbf{e}_{\mathrm{N}}, && (23)
\end{aligned}$$

since $\mathbf{N}$ is symmetric and idempotent, and $\mathbf{J}\mathbf{N} = \mathbf{N}\mathbf{J}^{\dagger} = \mathbf{0}$. Equation (23) is negative if $\mathbf{K}_{\mathrm{N}}$ is positive-definite, and hence $\dot{\mathbf{q}}$ converges to $\dot{\mathbf{q}}_{\mathrm{d}}$ in the space of $\mathbf{N}$.

5 Control Method for Torque Minimization with External Loading

In this section, a new control method is proposed to minimize the joint torques with forces on the manipulators end-effector. This method builds on the null space velocity control in Section 4.2. This ensures stability, and circumvents the fictitious damping forces in the null space damping method that interferes with the redundant task. Rather than locally minimize the total torque, as per the MKE method, the objective function is defined as a weighted sum. The first component is to minimize the norm of torques needed to oppose the forces on the end-effector. This is attenuated by the local dynamic torque. In this manner, the manipulator will align itself against the external force, but also minimize the effort required to achieve this.

5.1 Derivation of Desired Velocity, Acceleration

To stabilize the null space velocities, a desired joint velocity must be defined. In [23], the desired velocity was equivalent to the task for maximizing manipulability. Here, the desired velocity is constructed via the WLN solution to the differential kinematics (4). This way, both the main task and redundant task can be made to conform to physical constraints. The desired joint velocity and its time-derivative can be expressed generally as:

$$\dot{\mathbf{q}}_{\mathrm{d}} = \mathbf{J}_{\mathrm{W}}^{\dagger}\dot{\mathbf{x}} + \mathbf{N}_{\mathrm{W}}\dot{\mathbf{y}} \tag{24}$$

$$\ddot{\mathbf{q}}_{\mathrm{d}} = \mathbf{J}_{\mathrm{W}}^{\dagger}(\ddot{\mathbf{x}} - \dot{\mathbf{J}}\dot{\mathbf{y}}) + \dot{\mathbf{J}}_{\mathrm{W}}^{\dagger}(\dot{\mathbf{x}} - \mathbf{J}\dot{\mathbf{y}}) + \mathbf{N}_{\mathrm{W}}\ddot{\mathbf{y}}, \tag{25}$$

where the vector $\dot{\mathbf{y}}, \ddot{\mathbf{y}} \in \mathbb{R}^{\mathrm{n}}$ is formulated to minimize the joint torque $\boldsymbol{\tau}$. Note that multiplying (25) through by the Jacobian $\mathbf{J}$ gives $\mathbf{J}\ddot{\mathbf{q}}_{\mathrm{d}} = \ddot{\mathbf{x}} - \dot{\mathbf{J}}\dot{\mathbf{q}}_{\mathrm{d}}$, maintaining the kinematic constraints given by (3). To reiterate, it is possible to define $\dot{\mathbf{q}} = \dot{\mathbf{y}}$, but by using (24) the joints can be made to comply ith physical constraints through $\mathbf{J}_{\mathrm{W}}^{\dagger}$ (5).

By taking $\dot{\mathbf{y}}$ as proportional to the gradient vector of some scalar cost function $\mathrm{h}(\mathbf{q})$, (24) will optimize said cost function in the null space of the manipulator:

$$\dot{\mathbf{y}} = \alpha \nabla \mathrm{h}(\mathbf{q}), \tag{26}$$

where $\alpha < 0$ is a scalar that will minimize $\mathrm{h}(\mathbf{q})$. This is otherwise known as the Gradient Projection Method (GPM) [9]. Its time derivative is then:

$$\begin{aligned} \ddot{\mathbf{y}} &= \alpha \frac{\mathrm{d}}{\mathrm{dt}}\big(\nabla \mathrm{h}(\mathbf{q})\big) \\ &= \alpha \frac{\mathrm{d}}{\mathrm{d}\mathbf{q}}\big(\nabla \mathrm{h}(\mathbf{q})\big)\dot{\mathbf{q}} \\ &= \alpha \mathbf{H}(\mathbf{q})\dot{\mathbf{q}}, \end{aligned} \tag{27}$$

where $\mathbf{H}(\mathbf{q})$ is the Hessian of $\mathrm{h}(\mathbf{q})$.

To minimize the joint torques caused by a wrench on the end-effector, a cost function is defined as the weighted sum-of-squared torques from said wrench:

$$\mathrm{h}(\mathbf{q}) = \frac{1}{2}\boldsymbol{\tau}_{\mathrm{R}}^{\mathrm{T}}\mathbf{A}\boldsymbol{\tau}_{\mathrm{R}} \tag{28}$$

$$\nabla \mathrm{h}(\mathbf{q}) = (\partial \boldsymbol{\tau}_{\mathrm{R}}/\partial \mathbf{q})^{\mathrm{T}}\mathbf{A}\boldsymbol{\tau}_{\mathrm{R}} \tag{29}$$

$$\frac{\partial \mathrm{h}}{\partial \mathrm{q_j}} = \boldsymbol{\nu}_{\mathrm{i}}^{\mathrm{T}}\Big(\frac{\partial \mathbf{J}^{\mathrm{T}}}{\partial \mathrm{q_j}}\mathbf{R}_{\mathrm{i}} + \mathbf{J}^{\mathrm{T}}\frac{\mathbf{R}_{\mathrm{i}}}{\partial \mathrm{q_j}}\Big)^{\mathrm{T}}\mathbf{A}\mathbf{R}_{\mathrm{i}}\boldsymbol{\nu}_{\mathrm{i}}, \quad \mathrm{j} \in \{1, ..., \mathrm{n}\}. \tag{30}$$

Here, $\mathbf{A}$ is a positive-definite weighting matrix that can be used to give priority to joints with higher torque capacity or better mechanical advantage. The Hessian for (28) is difficult to calculate, so for practical purposes the change in $\nabla \mathrm{h}(\mathbf{q})$ over time is approximated using backwards differencing.

The joint motion in the redundant portion of the manipulator from $\dot{\mathbf{y}}, \ddot{\mathbf{y}}$ may locally increase the dynamic joint torque. Therefore, it can be reduced by considering the local acceleration caused by the torque components $\mathbf{c}$ and $\boldsymbol{\tau}_{\mathrm{R}}$:

$$\ddot{\mathbf{y}} = \alpha_1 \frac{\mathrm{d}}{\mathrm{dt}}\big(\nabla \mathrm{h}(\mathbf{q})\big) - \alpha_2 \mathbf{M}^{-1}(\mathbf{c} + \boldsymbol{\tau}_{\mathrm{R}}). \tag{31}$$

This appended term is similar to the MKE method (14). The velocity $\dot{\mathbf{y}}$ necessary for (25) can be calculated through discrete-time integration. Equation (31) is thus a weighted sum between minimizing the norm of $\boldsymbol{\tau}_{\mathrm{R}}$ and reducing the local dynamic torque. The scalars α_1 and α_2 can then be chosen based on the relative magnitude of the corresponding torques.

5.2 Incorporation of Physical Constraints

The control equations (4), (24), and (25) represent a weighted-least-norm solution for the joint motion. It is possible to account for physical constraints in the solution via the construction of the weighting matrix $\mathbf{W}$. Some examples include joint limit avoidance [18], self-collision avoidance [19], and obstacle avoidance [20]. In this paper, $\mathbf{W}$ is constructed for joint limit avoidance as per [18]. The weighting matrix is modified using the following cost function:

$$\mathrm{d}(\mathrm{q_i}) = \frac{(\mathrm{q_{i,max}} - \mathrm{q_{i,min}})(2\mathrm{q_i} - \mathrm{q_{i,max}} - \mathrm{q_{i,min}})}{\gamma_{\mathrm{i}}(\mathrm{q_{i,max}} - \mathrm{q_i})^2(\mathrm{q_i} - \mathrm{q_{i,min}})^2}, \tag{32}$$

in which magnitude of this function grows to infinity near joint limits, causing joints to slow down in their approach. In this paper, the joint limit cost function is combined with the inertia matrix $\mathbf{M}$:

$$\mathbf{W}_{\mathrm{ij}} = \mathbf{M}_{\mathrm{ij}} \qquad \forall \mathrm{i} \neq \mathrm{j} \tag{33}$$

$$\mathbf{W}_{\mathrm{ii}} = \begin{cases} \mathbf{M}_{\mathrm{ii}} + |\mathrm{d}(\mathrm{q_i})| & \mathrm{for} \Delta \mathrm{d}(\mathrm{q_i}) > 0 \\ \mathbf{M}_{\mathrm{ii}} & \mathrm{otherwise} \end{cases} \tag{34}$$

The inertia component of this weighting matrix will help minimize the kinetic energy in the manipulator. Furthermore, the element $\mathbf{W}_{\mathrm{ii}}$ will approach infinity as a joint moves toward its limit. Thus through (24) and (25), joints moving away from their limits will be given preference in the solution.

6 Case Studies

The proposed control method is examined through two different case studies. The first involves a manipulator lifting and moving a heavy object. Here, the manipulator must overcome gravitational forces when raising the object, but must also maintain a controlled descent when lowering it. Additionally, the object is inertially coupled with the manipulator and dynamic forces must be accounted for while moving. The second scenario involves robotic high-pressure blasting where the nozzle reaction forces continually push back against the manipulator. Furthermore, the direction of these forces changes depending on where the nozzle points as required by the task.

6.1 Case Study 1: Torque Minimization for Heavy Lifting

Table 1: Physical properties of the 7DOF manipulator used for the heavy-lifting simulation.

	Joint						
	1	2	3	4	5	6	7
Mass (kg)	5.3	4.5	1.7	2.5	1.1	1.6	0.3
Max. Torque (N)	80	80	40	40	9	9	9

Table 2: Parameters used in the simulation of heavy-lifting

	Parameter						
	$\mathrm{F_R}$	Frame	$\mathbf{A}$	α_1	α_2	$\mathbf{K_N}$	β
Value	60N	$\{0\}$	$\mathbf{I}$	$-10 \times \mathrm{F_R}^{-2}$	0.05	4	1
Equation	(35)	(12)	(28)	(31)	(31)	(17)	(15)

Outline: In this first case study, a dynamic model of the Sawyer robot by Rethink Robotics with 7DOF is simulated. The task requirement here is to lift a heavy object to a height of 650mm, move it 700m laterally, then lower it back down. The wrench on the end-effector is then denoted with respect to the base frame $\{0\}$:

$$\boldsymbol{\nu}_0 = \begin{bmatrix} 0 & 0 & \mathrm{F_R} & 0 & 0 & 0 \end{bmatrix}^{\mathrm{T}}. \tag{35}$$

As such, $\mathbf{R} = \mathbf{I}$ (12) and $\partial \mathbf{R}/\partial \mathrm{q_j} = \mathbf{0}$ (30). The joint torques generated by the weight of the object on the joints is then:

$$\boldsymbol{\tau}_{\mathrm{R}} = \mathbf{J}^{\mathrm{T}} \boldsymbol{\nu}_0. \tag{36}$$

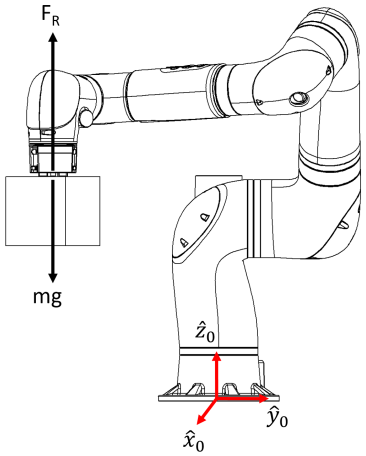

Fig. 1: When lifting, the manipulator must generate a force opposite the payload's gravitational force.

The object being lifted is also inertially coupled with the manipulator itself. This will introduced additional dynamic torques in the manipulator that must be balanced against the torque minimization from the external loading. Table 1 gives some of the physical properties of the manipulator used in the case study. Table 2 gives the parameters used in the control equations. The weight of the object is taken as $\mathrm{F_R} = 60N$ (6kg) which is 1.5 times greater than the nominal payload capacity [24].

Results: Fig. 3. shows a plot of the sum of the absolute joint torques for the lifting scenario. The method of torque minimization proposed in this paper reduces the total torque required for the task compared to the MKE method. Fig. 2. shows screenshots of an animation for the lifting task. From 1s to 3s, the manipulator brings joint 4 up over itself to reduce torque. As the manipulator moves the object sideways (6s to 9s), joints 1 and 2 move to bring joint 3 under the payload, resulting in a distinct drop in torque on joint 2 as can be seen in Fig. 4a. Since this arm

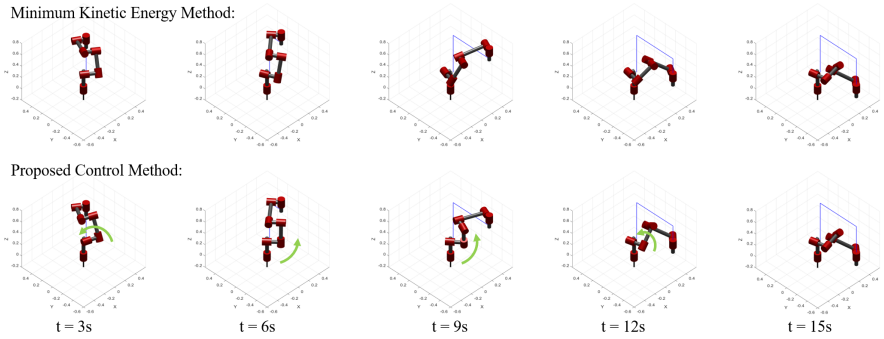

Fig. 2: Screenshots from the heavy-lifting simulation. At t=3s, the manipulator brings joint 4 up and over the payload to assist in lifting. From 6s to 9s, joint 3 is brought under the payload, resulting in a reduction in torque on joint 2 (Fig. 4a).

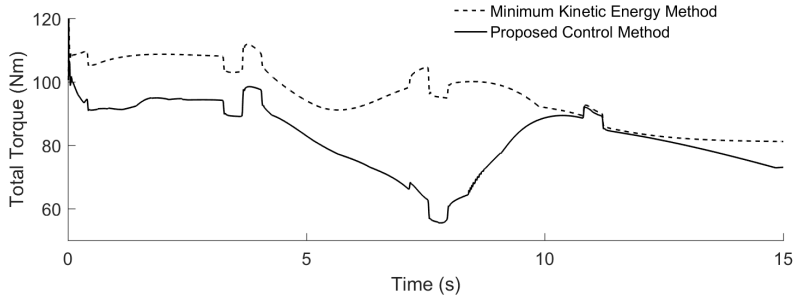

Fig. 3: Sum of absolute joint torques for the heavy-lifting case study. The proposed control method reduces the overall torque required for the task.

has larger tolerances on the joint torques and joint angles, neither control method exceeded limits.

6.2 Case Study 2: Torque Minimization for Robotic High-Pressure Blasting

Outline: In the second case study, a 6DOF manipulator is considered for high-pressure blasting of a flat surface. By exploiting some of the task properties, the manipulator can be tricked in to performing as a 9DOF system. A nozzle is mounted on the 6th link, in which the nozzle outlet is coincident with frame {6} in the kinematic model (Fig. 5a). The manipulator is required to direct the fluid stream at a location on a surface with a precise offset distance for optimal cleaning. Therefore, it is convenient to denote a virtual end-effector at the optimal cleaning point offset from {6}. Also, some leniency is tolerable in the orientation of this virtual end-effector. Thus, a virtual ball joint can be appended to the model, giving an additional 3DOF for a total of 9DOF. This also has the added advantage that the angle of attack of the working fluid with respect to the surface may be controlled.

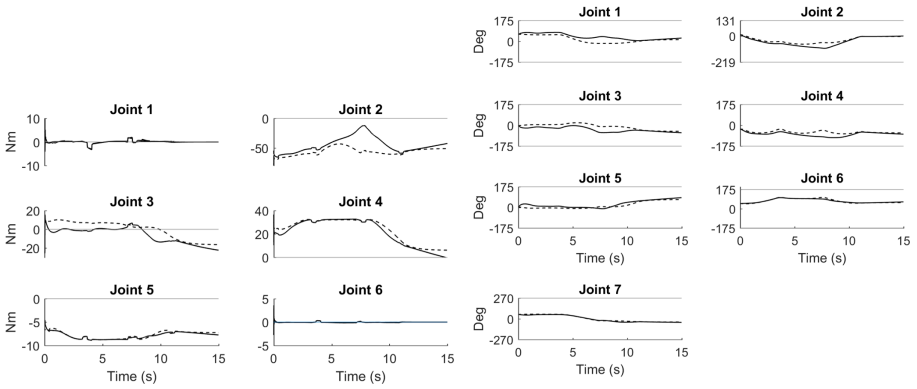

(a) Plot of individual joint torques. (b) Plot of individual joint angles.

Fig. 4: Joint torques and angles for the heavy-lifting simulation. The proposed control method rearranges the joints to reduce joint torque, and assist with lifting a heavy object.

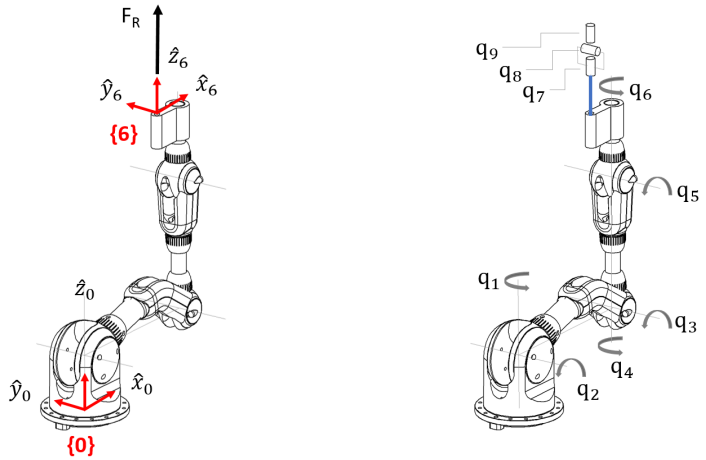

(a) Reference frames on the robot. (b) Real and virtual joints.

Fig. 5: (a) When blasting, the manipulator must generate a force along the z-axis of frame {6} to oppose the nozzle reaction forces. (b) The blasting point can be modelled with a virtual ball joint, givin an addtional 3DOF to the system.

Table 3: Physical properties of the 6DOF manipulator used for the heavy-lifting simulation.

	Joint					
	1	2	3	4	5	6
Mass (kg)	0.57	0.87	0.12	0.27	0.12	0.35
Max. Torque (N)	10	20	12	5	12	5

Table 4: Parameters used in the simulation of robotic blasting

	Parameter						
	F_R	Frame	$\mathbf{A}$	α_1	α_2	$\mathbf{K}_N$	β
Value	30N	{6}	$\mathbf{I}$	$-4 \times {F_R}^{-2}$	0	5	2
Equation	(38)	(12)	(28)	(31)	(31)	(17)	(15)

It should be noted that joints q_7, q_8 and q_9 are virtual and hence have no mass. As such, $\text{rank}(\mathbf{M}) = 6$ and the inertia matrix cannot be inverted. It is possible to add miniscule values to the diagonal elements $\mathbf{M}_{ii}$ for $i \in \{7, 8, 9\}$ to enable inversion of $\mathbf{M}$ without any noticeable effects on system performance. However, if one of the virtual joints is near its limit, then the weighting matrix as defined in (33),(34) becomes ill-conditioned. Since the inertia of this manipulator is small (Table 3), for this scenario it is sufficient to define the weighting matrix $\mathbf{W}$ as:

$$\mathbf{W}_{ii} = \begin{cases} 1 + |d(q_i)| & \text{for} \Delta d(q_i) > 0 \\ 1 & \text{otherwise} \end{cases} \tag{37}$$

To oppose the nozzle reaction forces F_R, the manipulator must generate a force along the positive z-axis of frame {6} (Fig. 5). Hence the wrench with respect to {6} is given as:

$$\boldsymbol{\nu}_6 = \begin{bmatrix} 0 & 0 & F_R & 0 & 0 & 0 \end{bmatrix}^T. \tag{38}$$

Then, from (11), the torque required to oppose the nozzle reaction forces is:

$$\boldsymbol{\tau}_R = \mathbf{J}^T \mathbf{R}_6 \boldsymbol{\nu}_6 \tag{39}$$

$$\mathbf{R}_6 = \begin{bmatrix} \mathbf{R}_0^6 & \mathbf{0}_{3\times3} \\ \mathbf{0}_{3\times3} & \mathbf{R}_0^6 \end{bmatrix}. \tag{40}$$

Since the payload capacity of the manipulator is much smaller than that used in [1-5], the nozzle reaction forces here are taken as $F_R = 30N$ (3kg). This is 6 times greater than the advertised payload capacity of the igus Robolink WR of 0.5kg [24], assuming the mechanical strength is greater than the joint torque limits.

For the task, the manipulator is required to trace a rectangle within its workspace 300mm wide and 150mm tall. In doing so, the initial and final pose of the end-effector are the same. It is expected, then, that the torque minimization method proposed in this paper will autonomously reconfigure the joints to reduce the overall torque once it returns to its starting position. As a baseline, the MKE method with null space damping (6c) is used to compare outcomes. Due to the low inertia of the manipulator $\|\boldsymbol{\tau}_R\| \gg \|\mathbf{M}\ddot{\mathbf{q}} + \mathbf{c}\|$ and the scalar $\alpha_2 = 0$ (31). The control parameters were manually adjusted to achieve desirable outcomes (Table 4).

Results: From the simulation results, the torque minimization method proposed in this paper reduces the overall torque from an external load on the end-effector (Fig. 7). In contrast, the MKE method sometimes leads to configurations that amplify the torques $\boldsymbol{\tau}_R$ from this external loading. Furthermore, the MKE method appears to have different results depending on initial conditions. Fig. 7 shows a plot of the sum of absolute joint torques for 2 different initial joint configurations. In one case,

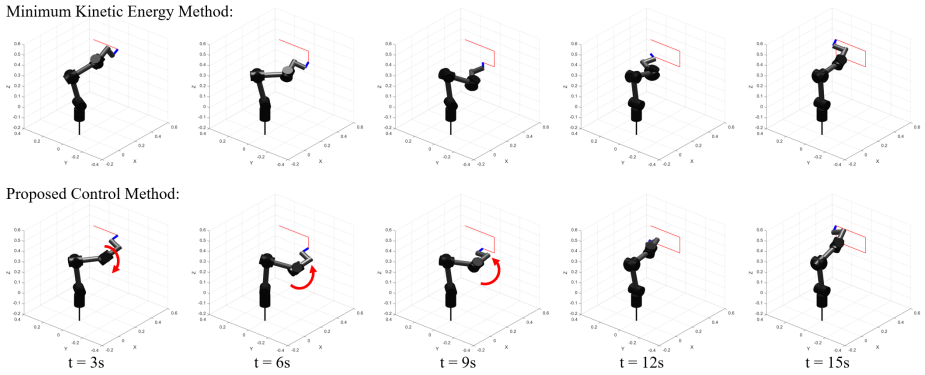

Fig. 6: Screenshots from the robotic blasting simulation. Using the proposed control method, the manipulator reconfigures itself to brace against the nozzle reaction forces.

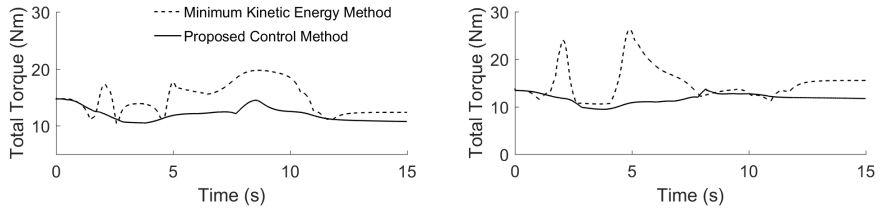

(a) Torque for a particular starting condition. (b) Torque with another starting condition.

Fig. 7: Sum of absolute joint torques for the blasting simulation. The MKE method increases the joint torque when an external load is applied. The proposes control method decreases the overall joint torque, for two different initial joint states.

the torque from the final configuration is larger than its starting conditions for the same end-effector pose.

The proposed control method, however, results in an overall reduction of torque for both initial states. In both situations, the joint torques converge to a similar result. Furthermore, in Fig. 8a it can be seen that the joint torques are sufficiently reduced to remain within torque limits (Table 3). Joint torques remained feasible even when the force on the end-effector was 6 times the nominal payload capacity. Fig. 8b compares joint angles using the MKE method and the proposed control method. The joint limits are violated using the MKE method for joints 5, 6 and 8. The method developed in this paper can simultaneously adhere to joint limits and minimize the overall torque as intended.

7 Discussion

7.1 Considerations and Limitations

Part of the redundant task (31) involves minimizing the norm of the torque vector $\boldsymbol{\tau}_{\mathrm{R}}$ that results from a wrench $\boldsymbol{\nu}$ on the end-effector (5b). However, there may

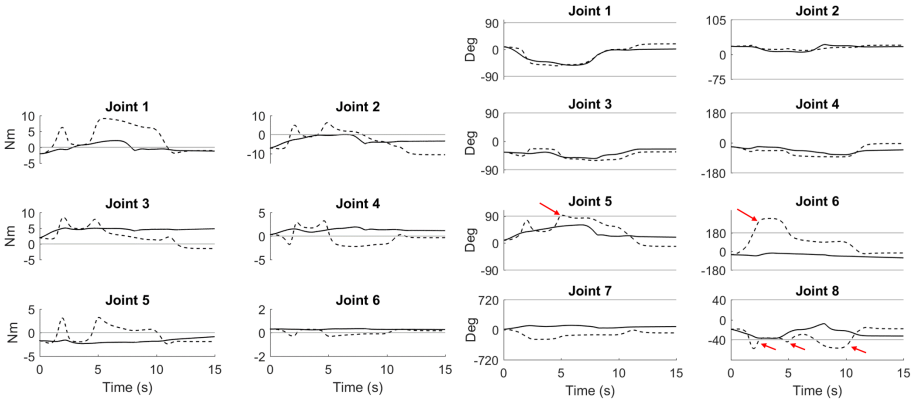

(a) Plot of individual joint torques.

(b) Plot of individual joint angles.

Fig. 8: Joint torques and joint angles for the robotic blasting simulation. The proposed control method is able to simultaneously reduce the joint torque required for the task, and avoid joint limits.

be situations in which we may want to utilize this force to assist in motion. The inclusion of the term $-\alpha_2 \mathbf{M}^{-1}\boldsymbol{\tau}_{\mathrm{R}}$ (31) performs this function to a degree, however (28) is working to minimize $\boldsymbol{\tau}_{\mathrm{R}}$. Consider the blasting scenario where we wish to clean a curved surface. We may want to stiffen the manipulator when moving forward in the direction of the nozzle to reduce torque, but relax the manipulator when moving back to take advantage of the nozzle reaction forces.

Furthermore, the redundant task (27) is defined by the gradient to the cost function (28). This will cause the joint state of the manipulator to converge to a local minimum of this function. The joint state here may not be adequate given the task requirements, even though a better local or global minimum may exist. Therefore, the secondary task may not be able to achieve a joint configuration that sufficiently minimizes the joint torque for the task and payload required. Nevertheless, the simulations showed good results, particularly with the blasting scenario in which the manipulator was constrained by relatively narrow joint limits and large end-effector forces.

Lastly, there is also the matter of choosing adequate control parameters for α_1, α_2, and $\mathbf{K}_{\mathrm{N}}$. In this paper, these values were manually adjusted to achieve desirable results. As such, large changes to the task requirements (i.e. end-effector velocity/acceleration, magnitude of the wrench) may not produce the same outcomes without further adjustment. However, this heuristic approach could be better addressed by considering the magnitude of the torque components, $\|\boldsymbol{\tau}_{\mathrm{R}}\|$, $\|\mathbf{x}\|$ to determine weighting coefficients α_1 and α_2 (31).

7.2 Mathematical Relationship to Cartesian Stiffness Control

Cartesian stiffness control is a prominent method for minimizing the deflection of the end-effector when subject to external forces [26-30]. Given a desired end-effector stiffness, often specified with respect to the base frame, a subsequent joint configuration can be optimized [28-30]. This inverse kinematics approach implies

that the either the manipulator is static, or the motion is pre-planned in the joint space.

Conversely, in this paper a torque minimization approach was proposed for real-time control of a manipulator, capable of trajectory tracking. However, there exists some mathematical relationships between this and Cartesian stiffness control that may be an avenue of future investigation.

In Cartesian stiffness control, the convention is to define a Cartesian stiffness matrix $\mathbf{K}_\mathrm{c}$, which maps a deflection of the end-effector $\Delta\mathbf{x}$ to a wrench $\boldsymbol{\nu}$:

$$\Delta\boldsymbol{\nu} = \mathbf{K}_\mathrm{c}\Delta\mathbf{x}. \tag{41}$$

Similarly, the deflection of the joints $\Delta\mathbf{q}$ is mapped to the (static) joint torques $\boldsymbol{\tau}_\mathrm{R}$ by the joint stiffness matrix $\mathbf{K}_\mathrm{q}$:

$$\Delta\boldsymbol{\tau}_\mathrm{R} = \mathbf{K}_\mathrm{q}\Delta\mathbf{q}. \tag{42}$$

Then from (9), (41), and(42):

$$\mathbf{K}_\mathrm{q}\Delta\mathbf{q} = \mathbf{J}^\mathrm{T}\Delta\boldsymbol{\nu} \tag{43}$$

$$\mathbf{K}_\mathrm{q}\Delta\mathbf{q} = \mathbf{J}^\mathrm{T}\mathbf{K}_\mathrm{c}\Delta\mathbf{x} \tag{44}$$

$$\mathbf{K}_\mathrm{q} = \mathbf{J}^\mathrm{T}\mathbf{K}_\mathrm{c}\mathbf{J}. \tag{45}$$

Equation (45) can be used to solve the necessary joint configuration/stiffness given $\mathbf{K}_\mathrm{c}$. It can be seen from (42) that:

$$\mathbf{K}_\mathrm{q} = \partial\boldsymbol{\tau}_\mathrm{R}/\partial\mathbf{q}, \tag{46}$$

and by re-examining the cost function (29) used to optimize the joint torques:

$$\nabla \mathrm{h}(\mathbf{q}) = \mathbf{K}_\mathrm{q}^\mathrm{T}\mathbf{A}\mathbf{J}^\mathrm{T}\boldsymbol{\nu}. \tag{47}$$

In (47), $\mathbf{J}^\mathrm{T}$ maps the wrench $\boldsymbol{\nu}$ from the task space to the joint space. The matrix $\mathbf{A}$ weights the torques, and the result is modulated by the joint stiffness $\mathbf{K}_\mathrm{q}$. That is, the redundant task will move the manipulator to increase the joint stiffness against the wrench. The Cartesian stiffness control and the torque minimization method presented here both involve the optimization of the joint stiffness. Therefore, the control method proposed in this paper could have the potential to achieve similar objectives. This may warrant further research.

8 Conclusion

Robotic manipulators are often required to undertake demanding tasks in which they must contend with various forces acting on the end-effector. The design selection of a manipulator is a careful balance of properties such as dexterity, workspace volume, degrees of freedom, and payload capacity. Given this, a manipulator may have to work at or above its payload capacity given constraints imposed on other properties due to the task requirements. In such a case, it is imperative that the joint configuration is carefully controlled to reduce joint torque.

Most methods in literature for joint torque minimization of redundant manipulators are formulated with respect to the internal dynamics of the system.

However, when external forces are applied to the end-effector, these methods may increase the overall joint torque. To address this issue, a method was proposed in this paper to minimize the overall joint torque where an external loading on the end-effector must be accounted for. This was applied through null space control, such that the joints can autonomously rearrange themselves and reduce the effects of the external force without affecting the end-effector. Furthermore, the proposed method factors in weighting on the joint motion which can be used to incorporate physical constraints on the solution.

Two case studies were considered to verify the proposed control method. In the first scenario, a manipulator was simulated lifting and moving a heavy object. In the second case study, a manipulator was simulated performing high-pressure blasting, where fluid reaction forces push back on the end-effector. Using the proposed control method, the overall joint torques were reduced compared to conventional methods. Furthermore, there is the added potential that a manipulator may work beyond its nominal payload capacity using this control method.

Acknowledgements Research supported in part by the Australian Research Council (ARC) Linkage Project (LP150100935) and the Roads and Maritime Services NSW.

References

1. D.K. Liu, G. Dissayanake, P. Manamperi, P. Brooks, G. Paul, S. Webb, N. Kirchner, P. Chotiprayanakul, N.M. Kwok, T. Ren, A Robotic System for Steel Bridge Maintenance: Research Challenges and System Design, Proceedings of the Australasian Conference on Robotics and Automation (ACRA) (2008)
2. Denso Wave Incorporated, 6-Axis robots VM series specifications (Online), (`http://www.denso-wave.com/en/robot/product/five-six/vm__Spec.html`) Accessed 12th Feb 2018
3. Paul, G., Webb, S.S., Liu, D. and Dissanayake, G., A robotic system for steel bridge maintenance: Field testing, Proceedings of the Australasian Conference on Robotics and Automation (ACRA), (2010)
4. P. Manamperi, P. Brooke, W. Kaluarachchi, G. Peters, A. Ho, S. Lie, A. To, G. Payl, D. Rushton-Smith, S. Webb, D.K. Liu, Robotic Grit-blasting: Engineering Challenges, Sustainable Bridges: The Thread of Society, pp. 321-330, (2011)
5. D.K. Liu, G. Dissanayake, J. Miro, K. Waldron, Infrastructure Robotics: Research Challenges and Opportunities, International Symposium on Automation and Robotics in Construction, vol. 31 p.1, (2014)
6. N. Kirchner, G. Paul, D.K. Liu, Bridge maintenance robotic arm: mechanical technique to reduce the nozzle force of a sandblasting rig, Journal of Wuhan University of Technology, Vol. 28, Suppl. 2006-083, 12-18, (2006)
7. J. Woolfrey, D.K. Liu, M. Carmichael, Kinematic Control of an Autonomous Underwater Vehicle-Manipulator System Using Autoregressive Predictive of Vehicle Motion and Model Predictive Control, IEEE International Conference on Robotics and Automation (ICRA), pp. 4591-4596, (2016)
8. P. Bhangale, V. Agrawal, S. Saha, Attribute based specification, comparison and selection of a robot, Proceedings of the 11th National Conference on Machines and Mechanisms, pp. 131-138, (2003)
9. T. Yoshikawa, Analysis and control of robot manipulators with redundancy, Robotics Research: The First International Symposium, Cambridge, MA, USA, pp. 735-747, (1984)
10. J. Hollerbach and K. Suh, Redundancy resolution of manipulators through torque optimization, IEEE Journal on Robotics and Automation 3(4), pp. 308-316, (1987)
11. A. Nedungadi and K. Kazerouinian, A local solution with global characteristics for the joint torque optimization of a redundant manipulator, Advanced Robotics vol. 6, no. 5, pp. 631-645, (1989)

12. H. Kang and R. Freeman, Joint torque optimization of redundant manipulators via the null space damping method, IEEE International Conference on Robotics and Automation, pp. 520-525, (1992)
13. C. Chung, B. Lee, M. Kim, C. Lee, Torque optimizing control with singularity-robustness for kinematically redundant robots, Journal of Intelligent and Robotic Systems, 28(3), pp. 231 258, (2000)
14. W. Tang and J. Wang, Two recurrent neural networks for local joint torque optimization of kinematically redundant manipulators, IEEE Transactions on Systems, Man, and Cybernetics, Part B (Cybernetics), 30(1), pp. 120-128, (2000)
15. Y. Zhang, S. Ge, T. Lee A unified quadratic-programming-based dynamical system approach to joint torque optimization of physically constrained redundant manipulators, IEEE Transactions on Systems, Man, and Cybernetics, Part B (Cybernetics), 34(5), pp. 2126-2132, (2004)
16. Y. Zhang, D. Guo, S. Ma, Different-level simultaneous minimization of joint-velocity and joint-torque for redundant robot manipulators, Journal of Intelligent and Robotic Systems, 72(3-4), pp. 301-324, (2013)
17. F. Flacco and A. De Luca, Discrete-time redundancy resolution at the velocity level with acceleration/torque optimization properties, Robotics and Autonomous Systems 70, pp. 191-201, (2015)
18. T. Chan, R. Dubey, A weighted least-norm solution based scheme for avoiding joint limits for redundant joint manipulators, IEEE Transactions on Robotics and Automation, 11(2), pp. 286-292, (1995)
19. B. Dariush, G.B. Hammam, D. Orin, Constrained Resolved Acceleration Control for Humanoid Robots, IEEE/RSJ International Conference on Intelligent Robots and Systems, pp. 710-717 , (2010)
20. P. Chen, C. Shan, J. Xiang, W. Wei, Moving Obstacle Avoidance for Redundant Manipulator via Weighted Least Norm Method, 27th Chinese Control and Decision Conference (CCDC), pp. 6181-6186, (2015)
21. C. Wampler, Manipulator Inverse Kinematic Solutions Based on Vector Formulations and Damped-Least-Sqaures Methods, IEEE Transactions on Systems, Man, and Cybernetics, SMC-16, No. 1, pp. 93-101, (1986)
22. S. Chiaverini, O. Egeland, R. Kanestrom, Achieving user-defined accuracy with damped least-squares inverse kinematics, Fifth International Conference on Advanced Robotics, pp. 672-677, (1991)
23. P. Hsu, J. Hauser, S. Sastry, Dynamic Control of Redundant Manipulators, Journal of Robotic Systems, 6(2), pp. 133-148, (1989)
24. Rethinkrobotics.com, Sawyer Technical Specifications, (Online)(`http://www.rethinkrobotics.com/sawyer/tech-specs/`), Accessed 5th Feb 2018
25. Igus.com, Robolink WR, (Online), (`https://www.igus.com/wpck/16962/N16_10_11`) , Accessed 5th Feb 2018
26. H.R. Choi, W.K. Chung, and Y. Youm, Stiffness analysis and control of redundant manipulators IEEE International Conference on Robotics and Automation (ICRA), pp. 689-695, (1994)
27. M.H. Ang and G.B. Andeen, Specifying and achieving passive compliance based on manipulator structure, IEEE Transaction on Robotics and Automation, 11(4), pp. 504-515, (1995)
28. Y. Li and L. Kao, Stiffness control on redundant manipulators: a unique and kinematically consistent solution, IEEE International Conference on Robotics and Automation (ICRA), pp. 3956-3961, (2004)
29. A. Ajoudani, N.G. Tsagarakis, and A. Bicchi, Ajoudani, A., Tsagarakis, N.G. and Bicchi, On the role of robot configuration in Cartesian stiffness control, IEEE International Conference on Robotics and Automation (ICRA), pp. 1010-1016, (2015)
30. G.M. Gasparri, F. Gabiani, M. Garabini, L. Pallottino, M. Catalon, G. Grioli, R. Perischin, and A. Bicchi, Robust optimization of system compliance for physical interaction in uncertain scenarios, IEEE-RAS 16th International Conference on Humanoid Robots (Humanoids), pp. 911-918, (2016)